LETTERS

Record of mid-Archaean subduction from metamorphism in the Barberton terrain, South Africa

Jean-François Moyen[1], Gary Stevens[1] & Alexander Kisters[1]

Although plate tectonics is the central geological process of the modern Earth, its form and existence during the Archaean era (4.0–2.5 Gyr ago) are disputed[1,2]. The existence of subduction during this time is particularly controversial because characteristic subduction-related mineral assemblages, typically documenting apparent geothermal gradients of $15\,^\circ C\,km^{-1}$ or less[3], have not yet been recorded from *in situ* Archaean rocks (the lowest recorded apparent geothermal gradients[4] are greater than $25\,^\circ C\,km^{-1}$). Despite this absence from the rock record, low Archaean geothermal gradients are suggested by eclogitic nodules in kimberlites[5,6] and circumstantial evidence for subduction processes, including possible accretion-related structures[2], has been reported in Archaean terrains. The lack of spatially and temporally well-constrained high-pressure, low-temperature metamorphism continues, however, to cast doubt on the relevance of subduction-driven tectonics during the first 1.5 Gyr of the Earth's history[7]. Here we report garnet–albite-bearing mineral assemblages that record pressures of 1.2–1.5 GPa at temperatures of 600–$650\,^\circ C$ from supracrustal amphibolites from the mid-Archaean Barberton granitoid-greenstone terrain. These conditions point to apparent geothermal gradients of 12–$15\,^\circ C$—similar to those found in recent subduction zones—that coincided with the main phase of terrane accretion in the structurally overlying Barberton greenstone belt[8]. These high-pressure, low-temperature conditions represent metamorphic evidence for cold and strong lithosphere, as well as subduction-driven tectonic processes, during the evolution of the early Earth.

Recent studies have highlighted the composite nature of the early- to mid-Archaean Barberton granitoid-greenstone terrain and have demonstrated that the deep crustal levels (30–40 km) are exposed in structurally bounded domains in the granitoid-gneiss terrain to the south of the shallow-crustal greenstone belt[9,10]. Sedimentological, structural and geochronological differences indicate that the belt is made up of a northern and a southern terrane that are separated by the central, NE–SW trending Saddleback–Inyoka fault. The amalgamation of these two proposed island-arc terranes occurred during the main, D2 phase of collisional tectonics at ~3.23 Gyr ago, probably in an arc-trench setting[8]. The surrounding, granitoid-greenstone terrain is made up of (1) an amphibolite-facies greenstone component, (2) mainly gneissic trondhjemitic plutonic rocks ~3.55–3.45 Gyr old, (3) syntectonic (D2) trondhjemites and tonalites ~3.23–3.22 Gyr old[11]. The older trondhjemites and the associated greenstone remnants form an extensive, relatively high-grade domain (the Stolzburg terrane, Fig. 1), that was metamorphosed to pressures of up to 8–11 kbar (refs 9, 10). Significantly, peak metamorphic conditions in the high-grade gneiss terrain were attained during the D2 phase of tectonism, coeval with the accretion of the two island-arc terranes in the shallow-crustal greenstone belt. In other words, the supracrustal greenstone belt and the deep-crustal gneiss terrain expose sections through different crustal levels of the ~3.23-Gyr collisional orogen.

This study presents the results of a metamorphic analysis of rare mineral assemblages found in supracrustal remnants from within a prominent shear zone within this gneiss terrain, the Inyoni shear zone, which is probably the mid- to lower crustal expression of the suture that accommodated the mid-Archaean terrane accretion. The Inyoni shear zone is an up to 3 km wide, north-trending subvertical belt of banded, often migmatitic gneisses (Fig. 1). It extends southwards, to the kilometre-scale amphibolite-facies Schapenburg Schist belt. In the west, it is intruded by syntectonic bodies of coarse-grained, leucocratic trondhjemites to granodiorites. Some of these D2 bodies yielded ages of 3.229 ± 0.005 Gyr (ref. 12) and 3.231 ± 0.005 Gyr (ref. 13), constraining the timing of the deformation. Towards the east, the zone is bounded by relatively homogeneous and lower-strain gneisses of the high-grade Stolzburg terrane. Although heterogeneous strain and high degrees of fabric transposition make it difficult to establish the overall kinematics and strain within the shear zone, the scarcity of non-coaxial fabrics and the fabric geometry point to a dominantly bulk flattening strain associated with a component of vertical extrusion of the rocks. The gneisses of the Inyoni shear zone contain metre- to kilometre-scale, variably deformed and metamorphosed metavolcanic and subordinate metasedimentary remnants. Lithological differences between mappable packages, both in the Inyoni shear zone proper, and in the Schapenburg Schist belt, together with contrasting pressure–temperature (*P–T*) conditions (8–11 kbar and 650–700 °C (ref. 14) in the North; ~5 kbar and 630 °C in Schapenburg) suggest that this composite gneiss belt is a tectonic melange, juxtaposing rocks from diverse crustal depths intruded by largely synkinematic granitoids. A northern metavolcanic package (Fig. 1) consists predominantly of layered, epidote- and hornblende-dominated amphibolites. Garnet occurs within specific, relatively iron-rich horizons and the metamorphic history of this zone can best be understood by focusing on these pressure-sensitive garnet-bearing assemblages.

Prograde metamorphic evolution is recorded in low-strain domains, such as the cores of rootless isoclinal folds, where garnet grew simultaneously with albitic plagioclase, as evidenced by euhedral garnets surrounded by plagioclase (Fig. 2a) or albitic inclusions within garnets, sometimes with negative garnet forms. Clinopyroxene and quartz are sometimes intergrown with garnet (Fig. 2b). This assemblage formed at the expense of a relatively sodic amphibole (Fe-edenite, up to 1.1 sodium atoms per formula unit), and epidote, partially reequilibrated relicts of which are found in crystallographic continuity within albitic moats around the garnets. Qualitatively, garnet–clinopyroxene–quartz assemblages are known to form at relatively high pressures[15]. In coexisting garnet–plagioclase pairs, Ca is preferentially partitioned into garnet over plagioclase as pressure increases[15]; thus, relatively calcic garnets coexist with sodic

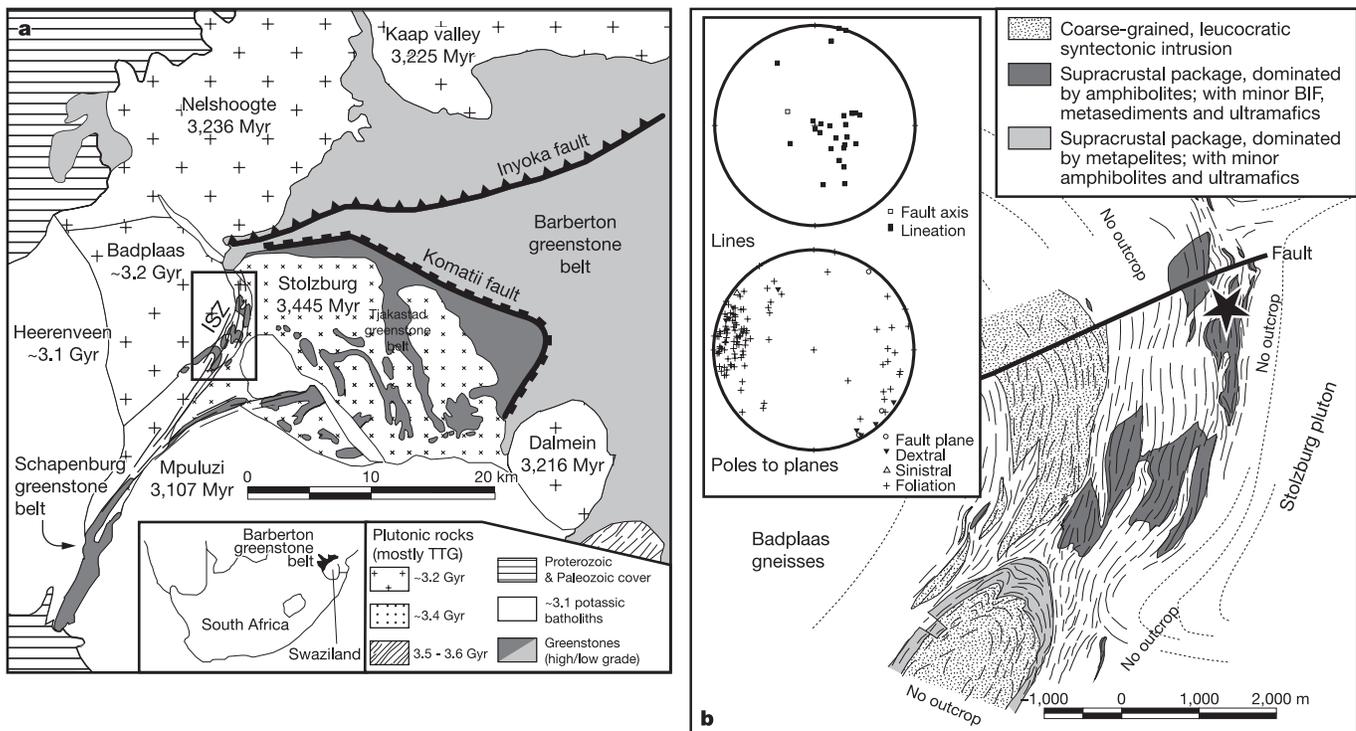[1]Department of Geology, University of Stellenbosch, South Africa Private Bag X-1, Matieland 7602, South Africa.

Figure 1 | Location of the Inyoni shear zone and studied samples in the southern Barberton terrane[14]. **a,** Regional geological map. Ages are from refs 11 and 21. ISZ, Inyoni shear zone. The box indicates the location of the detailed map in **b.** The darker-grey domain and the areas marked with smaller crosses correspond to the high-grade ~3.45-Gyr Stolzburg block. **b,** Detailed geological map of the northern Inyoni shear zone. The white background represents the felsic, trondhjemitic and tonalitic (TTG) gneisses. Dotted lines display foliation trends. BIF, banded iron formation. Inset, stereograms (Schmidt, lower hemisphere) for the central domains of the mapped area. The star in **b** denotes the location of the studied samples, which were derived from different amphibolite bodies.
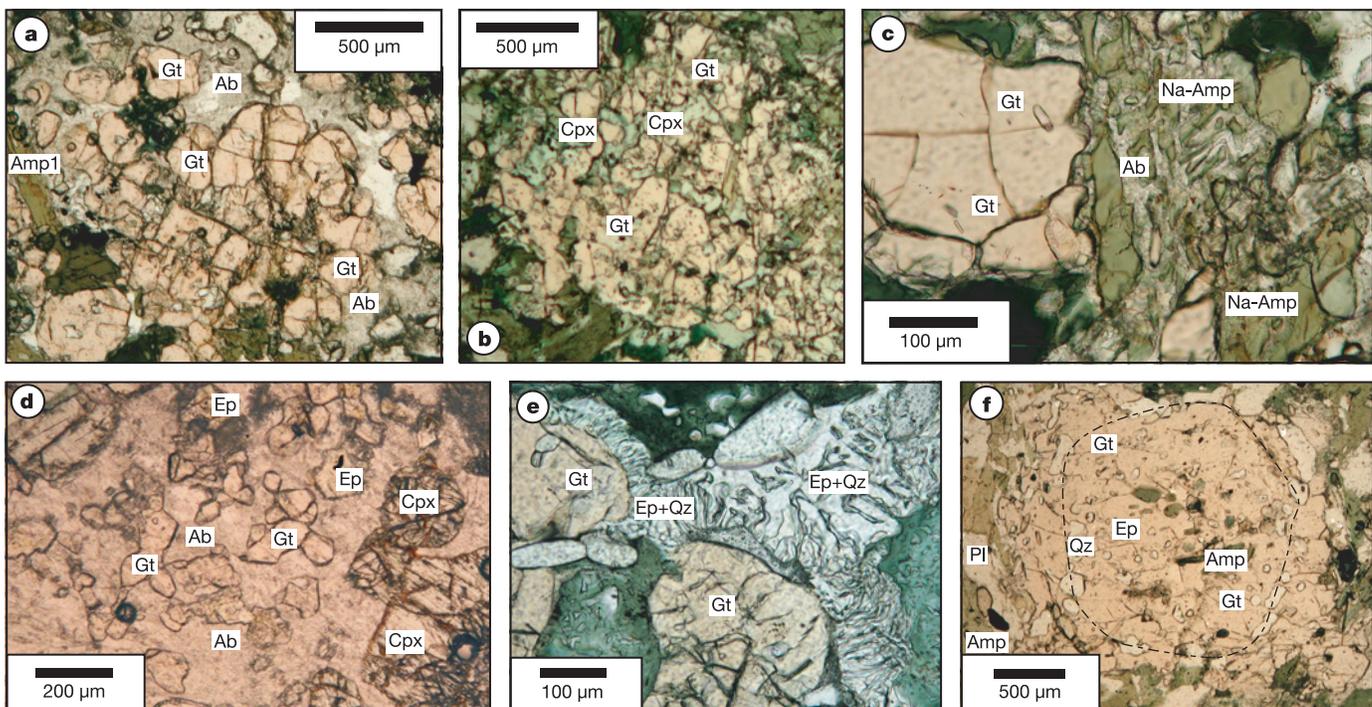

Figure 2 | Metamorphic textures associated with garnet growth or breakdown (plane-polarized light). a, Small euhedral garnets rimmed by albitic plagioclase, coalescing into large, poekilitic grains (INY131). **b,** Garnet–clinopyroxene intergrowth associated with garnet formation; the large garnet–clinopyroxene grain is rimmed by albite, not seen at this magnification (INY115). **c,** Breakdown of sodic amphibole within the albitic moats rimming garnets (INY131). **d,** Albitic plagioclase with euhedral grains of garnet and epidote, evidence of the breakdown of an earlier, more calcic plagioclase. **e,** Garnet surrounded by epidote–quartz symplectites (INY25). **f,** Core-to-rim zoned garnet, with a low-temperature core with albite, epidote and amphibole inclusions rimmed by a higher-temperature rim in equilibrium with more calcic plagioclase and amphibole; a ring of quartz inclusions bounds the core (dashed line) (INY21). Amp, amphibole (Amp1, early Na-rich amphibole); Pl, plagioclase (Ab, albitic plagioclase); Gt, garnet; Cpx, clinopyroxene; Ep, epidote; Qz, quartz.
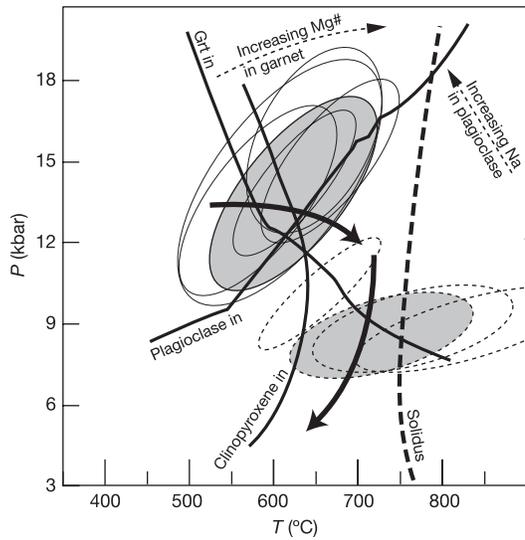
Figure 3 | THERMOCALC *P–T* estimates for garnet growth and breakdown sites in the studied samples. Filled ellipses are the average for 11 (garnet growth, solid lines) and 9 (garnet breakdown, dashed lines) sites; empty ellipses are examples of individual calculations, each corresponding to one single reaction site using the compositions of minerals in textural equilibrium. Different mineral assemblages were used (for example, garnet–clinopyroxene–plagioclase–quartz, and garnet–amphibole–plagioclase–epidote–quartz, for the garnet growth sites); they all produce indistinguishable *P–T* estimates within error. Imprecision associated with the plagioclase activity model, especially for low-An contents[22], creates a relative error on An activity of 5–15% in garnet growth sites (low-An plagioclase) and 2–5% in garnet breakdown sites (intermediate plagioclase composition). An additional source of error is that inherent to the calibration of the garnet–clinopyroxene–plagioclase–quartz barometer[22]. These uncertainties are integrated within the THERMOCALC *P–T* estimates[23,24]. Despite the significant error ellipses, the uncertainty on the apparent geotherm is much lower, owing to the positive slope of the reactions used in *P–T* estimates.

plagioclase at the highest pressures of plagioclase-and-garnet co-existence (Fig. 3). The prograde garnet generation documented in this study is indeed calcic (35–40% grossular) and coexists with almost pure sodic endmember albitic plagioclase ($An_{3–10}$). The garnet-in reaction is steeply oriented in *P–T* space in the area where it intersects the high-pressure plagioclase phase boundary. The magnesium number Mg# (Mg/Mg + Fe) in garnet scales inversely with temperature away from this phase boundary. The low Mg# (10–15) of the prograde garnet in these rock compositions (Mg# ≈ 50) argues for

low-temperature garnet formation (Fig. 3). This approach is confirmed by estimates using THERMOCALC[16] thermobarometry (analytical techniques and representative mineral estimates are given in Supplementary Tables 1 and 2, respectively), consistently pointing to conditions of formation of 12–15 kbar and 600–650 °C (Fig. 3) for the garnet-bearing assemblage. Garnet from samples in the high-strain domains (samples INY 25, 591a) generally shows retrograde textures (Fig. 2e). Garnet breakdown conditions, recorded by epidote + Fe-tschermakite + quartz symplectite coronas around
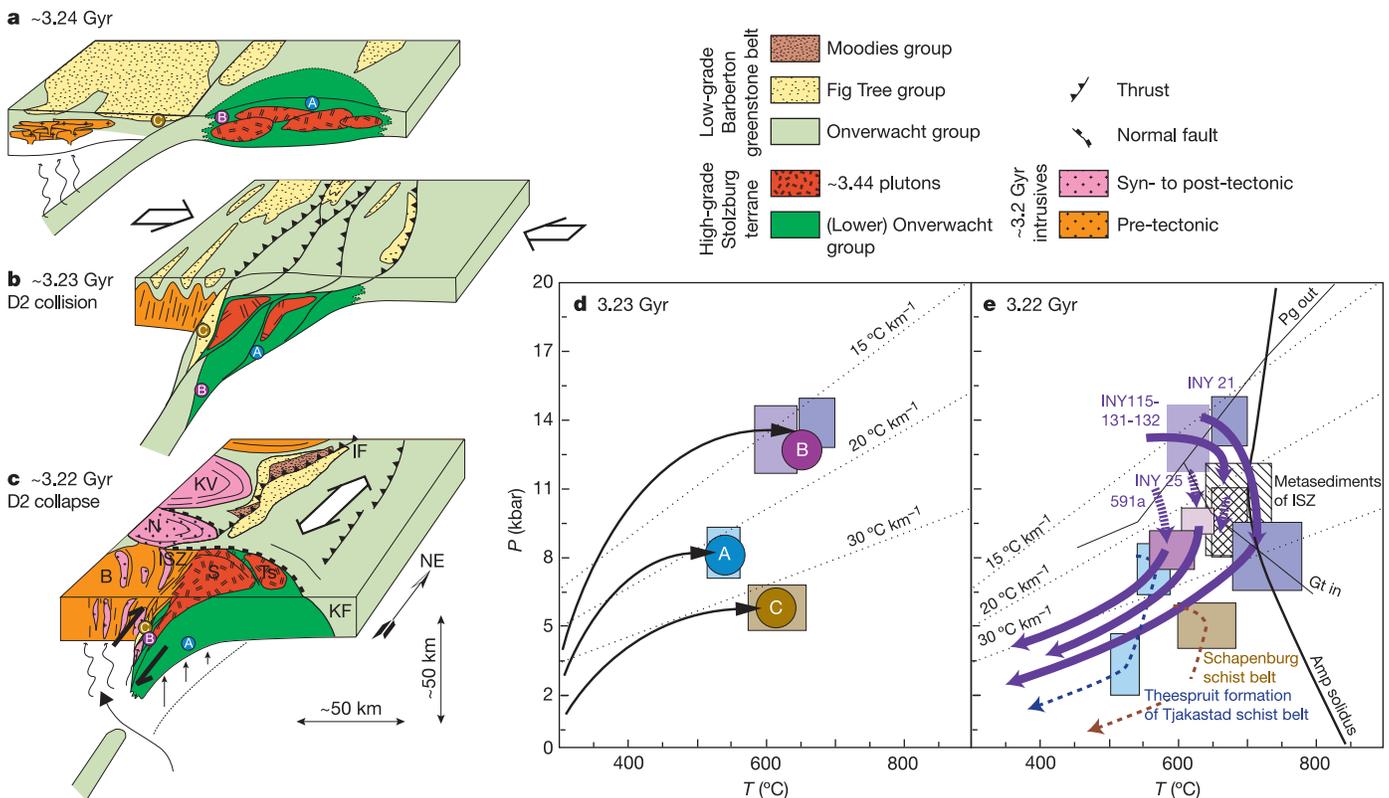

Figure 4 | Geodynamic sketch summarizing the inferred tectonic evolution of the southern Barberton terrane, and the associated metamorphic evolution. a–c, Circles lettered A, B and C correspond to the Theespruit (Ts) formation of the Tjakastad schist belt[10], the ISZ samples from this study, and the Schapenburg greenstone belt[13], respectively. IF, Inyoka fault; KF, Komatii fault. Plutons are: Ts, Theespruit; KV, Kaap valley; N, Nelshoogte; B, Badplaas; S, Stolzburg. **d, e,** The *P–T* of points A, B and C during the assembly and collapse phases of the orogen are shown. The two hatched blocks marked 'metasediments of ISZ' in **e** are from ref. 9.

the garnets, correspond to (THERMOCALC) temperatures of 580–650 °C at 8–10 kbar. This set of metamorphic conditions is consistent with the position of the (negatively sloped) garnet phase boundary in this part of the *P–T* space (Fig. 3); the estimated metamorphic conditions from these decompression structures corresponds well with peak metamorphic estimates from the nearby clastic sedimentary intercalations within the metavolcanic sequence[9]. The peak pressure *P–T* estimates are at present the highest crustal pressures reported for Archaean rocks, and correspond to by far the lowest known apparent geothermal gradients ($\sim 12\,°C\,km^{-1}$) in the Archaean rock record. In the modern Earth, the only process capable of producing crustal rock evolution through this *P–T* domain occurs within subduction zones.

The Inyoni shear zone is the structurally and lithologically composite western boundary of the structurally coherent, high-pressure, low-temperature Stolzburg granitoid-gneiss terrane. The presence of rocks with a high-pressure history consistent with a subduction origin in this zone suggests that this may conceivably represent the suture along which the high-grade continental Stolzburg terrane was rapidly buried to depths of at least 35–40 km (Fig. 4) (refs 9, 17). We suggest that the mélange-like character of the shear zone is the result of the structural imbrication of deeply buried slivers during the buoyancy-assisted return flow between or close to the downgoing slab and the overriding plate[18]. The abundance of synkinematic trondhjemites in the shear zone is likely to be the result of decompression melting of amphibolites during the retrograde exhumation path. The presence of these melts is possibly important to understanding the documented metamorphic signature. High-strain fabrics confined to synkinematic trondhjemites point to strain localization into the melts, which, in turn, is likely to assist the buoyancy- or extrusion-related exhumation of the rocks. The advective heat transfer associated with the intrusion of these synkinematic magmas also contributes to the syn- to late-collisional heat budget of the collisional belt that acted to partially destroy the evidence for the earlier high-pressure, low-temperature metamorphism. In many respects, this is similar to high-pressure amphibolites from more recent subduction–collision belts, which often occur as partially retrogressed boudins within migmatites[19,20]. Our findings of high-pressure, low-temperature metamorphic mineral assemblages from an active margin setting strongly suggest that lithospheric subduction was functioning as early as 3.2 Gyr ago before present.

1. Hamilton, W. B. Archean magmatism and deformation were not products of plate tectonics. *Precambr. Res.* **91**, 143–179 (1998).
2. de Wit, M. J. On Archaean granites, greenstones, cratons and tectonics: does the evidence demand a verdict? *Precambr. Res.* **91**, 181–226 (1998).
3. Ernst, W. G. Tectonic history of subduction zones inferred from retrograde blueschist P-T paths. *Geology* **16**, 1081–1084 (1988).
4. Riciputi, L. R., Valley, J. W. & McGregor, V. R. Conditions of Archean granulite-facies metamorphism in the Gothåb-Fiskenaesset region, southern West Greenland. *J. Metamorph. Geol.* **8**, 171–190 (1990).
5. Rollinson, H. Eclogite xenoliths in West African kimberlites as residues from Archaean granitoid crust formation. *Nature* **389**, 173–176 (1997).
6. Ireland, T. R., Rudnick, R. L. & Spetius, Z. Trace elements in diamond inclusions from eclogites reveal link to Archaean granites. *Earth Planet. Sci. Lett.* **121**, 199–213 (1994).
7. Bjørnerud, M. G. & Austrheim, H. Inhibited eclogite formation: the key to the rapid growth of strong and buoyant Archean continental crust. *Geology* **32**, 765–768 (2004).
8. De Wit, M. J. *et al.* Formation of an Archaean continent. *Nature* **357**, 553–562 (1992).
9. Dziggel, A., Stevens, G., Poujol, M., Anhaeusser, C. R. & Armstrong, R. A. Metamorphism of the granite–greenstone terrane south of the Barberton greenstone belt, South Africa: an insight into the tectono-thermal evolution of the 'lower' portions of the Onverwacht group. *Precambr. Res.* **114**, 221–247 (2002).
10. Diener, J., Stevens, G., Kisters, A. F. M. & Poujol, M. Metamorphism and exhumation of the basal parts of the Barberton greenstone belt, South Africa: constraining the rates of mid-Archaean tectonism. *Precambr. Res.* **143**, 87–112 (2005).
11. Kamo, S. L. & Davis, D. W. Reassessment of Archean crustal development in the Barberton mountain land, South-Africa, based on U-Pb dating. *Tectonics* **13**, 167–192 (1994).
12. Dziggel, A., Armstrong, R. A., Stevens, G. & Nasdala, L. Growth of zircon and titanite during metamorphism in the granitoid-gneiss terrain south of the Barberton greenstone belt, South Africa. *Mineral. Mag.* **69**, 1021–1038 (2006).
13. Stevens, G., Droop, G. T. R., Armstrong, R. A. & Anhaeusser, C. R. Amphibolite-facies metamorphism in the Schapenburg schist belt: a record of the mid-crustal response to ~3.23 Ga terrane accretion in the Barberton greenstone belt. *S. Afr. J. Geol.* **105**, 271–284 (2002).
14. Kisters, A. F. M., Stevens, G., Dziggel, A. & Armstrong, R. A. Extensional detachment faulting and core-complex formation in the southern Barberton granite–greenstone terrain, South Africa: evidence for a 3.2 Ga orogenic collapse. *Precambr. Res.* **127**, 355–378 (2003).
15. Kohn, M. J. & Spear, F. S. Empirical calibration of geobarometers for the assemblage garnet + hornblende + plagioclase + quartz. *Am. Mineral.* **74**, 77–84 (1989).
16. Holland, T. J. B. & Powell, R. An internally consistent thermodynamic dataset for phases of petrological interest. *J. Metamorph. Geol.* **16**, 309–343 (1998).
17. Diener, J. F. A., Stevens, G. & Kisters, A. F. M. High-pressure low-temperature metamorphism in the southern Barberton granitoid-greenstone terrain, South Africa: a record of overthickening and collapse of mid-Archean continental crust. In *Archean Geodynamics And Environments* (eds Benn, K., Mareschal, J.-C. & Condie, K.) 239–354 (AGU Geophysical Monograph Series Vol. 164, AGU, Washington, 2005).
18. Chemenda, A. I., Mattauer, M. & Bokun, A. N. Continental subduction and a mechanism for exhumatin of high-pressure metamorphic rocks: new modelling and field data from Oman. *Earth Planet. Sci. Lett.* **143**, 173–182 (1996).
19. Nicollet, C. & Leyreloup, A. Pétrologie des niveaux trondjhémitiques de haute pression associés aux éclogites et amphibolites des complexes leptyno amphiboliques du Massif Central français. *Can. J. Earth Sci.* **15**, 695–707 (1978).
20. Bodinier, J. L., Burg, J.-P., Leyreloup, A. & Vidal, H. Reliques d'un bassin d'arriere arc subducté puis obducté dans la région de Marvejols (Massif Central). *Bull. Soc. Geol. Fr.* **8**, 20–34 (1988).
21. de Ronde, C. E. J. & Kamo, S. L. An Archaean arc-arc collisional event: a short-lived (ca 3 Myr) episode, Weltvreden area, Barberton greenstone belt, South Africa. *J. Afr. Earth Sci.* **30**, 219–248 (2000).
22. Spear, F. S. *Metamorphic Phase Equilibria and Pressure-Temperature-Time Paths* 535 (Mineralogical Society of America, Washington, 1993).
23. Powell, R., Holland, T. J. B. & Worley, B. Calculating phase diagrams involving solid solutions via non-linear equations, with examples using THERMOCALC. *J. Metamorph. Geol.* **16**, 577–588 (1998).
24. Holland, T. J. B. & Blundy, J. Non-ideal interactions in calcic amphiboles and their bearing on amphibole-plagioclase thermometry. *Contrib. Mineral. Petrol.* **116**, 433–447 (1994).